RSC Advances

ROYAL SOCIETY OF CHEMISTRY

www.rsc.org/advances

Graphical Abstract

Unprecedented ferrocene-quinoline conjugates: facile proton conduction *via* 1D helical water chains and selective chemosensor for Zn(II) ion in water

Joseph Ponniah S[a], Subrat Kumar Barik[a], Rosmita Borthakur[a], Arunabha Thakur[a], Bikash Garai[b], Sourita Jana[a] and Sundargopal Ghosh[a]*

Absorption of water by a ferrocene-quinoline conjugate shows H-bonded 3D-networks of water in the molecular pockets and acts as an efficient proton conductor.

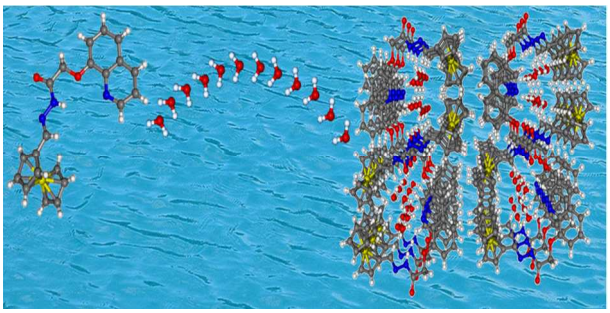

Cite this: DOI: 10.1039/c0xx00000x

www.rsc.org/xxxxxx

ARTICLE TYPE

Unprecedented ferrocene-quinoline conjugates: facile proton conduction *via* 1D helical water chains and selective chemosensor for Zn(II) ion in water

Joseph Ponniah S[a], Subrat Kumar Barik[a], Rosmita Borthakur[a], Arunabha Thakur[a], Bikash Garai[b], Sourita Jana[a] and Sundargopal Ghosh[a]*

Received (in XXX, XXX) Xth XXXXXXXXX 20XX, Accepted Xth XXXXXXXXX 20XX
DOI: 10.1039/b000000x

Two novel ferrocene-quinoline derivatives 3 ($C_{22}H_{19}O_2N_3Fe$) and 4 ($C_{34}H_{28}O_4N_6Fe$) have been synthesized and structurally characterized. Compound 3 exhibits good proton conductivity through 1D helical water chain. In addition, both compounds 3 and 4 selectively detect Zn^{2+} ion in water with a detection limit of 2 ppb through multiple channel.

Proton-conductivity studies are an emerging area of interest for their potential applications in transport dynamics, electrochemical devices and fuel cells.[1] Designing new proton conducting materials capable of operating under low humidity or anhydrous conditions and at high temperature are extremely important and have been an active task for synthetic chemists.[2] Currently, proton conduction materials are mostly based on sulfonated polymers such as Nafion, which show very low proton conductivity at high temperature.[3] Few attempts have been made to transform several inorganic and organic materials to proton conducting for their potential applications in fuel cells and sensors.[4] Metal organic frameworks (MOFs) due to their diverse topological architecture have been explored as potential materials for proton conduction.[5] Kitagawa, Banerjee and others have broadly studied the proton conductivity in various MOFs, where water or five-membered aza-heterocycles have played a vital role for this purpose. [5,6] However, till date, not much development has been made in this area that may offer advanced applications at lower cost, higher efficiency, or different operating conditions.[7]

Small and easily accessible organic–inorganic compounds are viable candidates for the investigation of proton carriage due to their structural diversity and porosity.[8] The introduction of suitable components within the molecule drives the proton transport phenomena.[9] Among them, water clusters are of great interest due to their 1D helical arrangement inside the host molecular domain through hydrogen bonding network.[10] Ferrocene in amalgamation with other molecules have found its importance in many synthetic materials due to their ideal electrochemical properties and stability in aqueous media.[11] On the other hand, the presence of nitrogen containing heterocycles also improves the proton conductivity of the material.[12,13] Thus, introduction of a quinoline moiety into one of the ferrocene rings may exhibit good proton conducting properties.[14]

In continuation of our work on ferrocene based molecules,[15,16] we present in this communication two novel unprecedented ferrocene-quinoline conjugates **3** and **4** synthesized by a simple "*Schiff-base*" condensation reaction of 2-(quinolin-8-yloxy)acetohydrazide with ferrocene mono aldehyde and 1,1' ferrocene di-aldehyde respectively (Scheme S1)†. Both the conjugates **3** and **4** are characterized by multinuclear NMR, ESI mass spectrometry and X-ray diffraction studies (detail in SI)†.

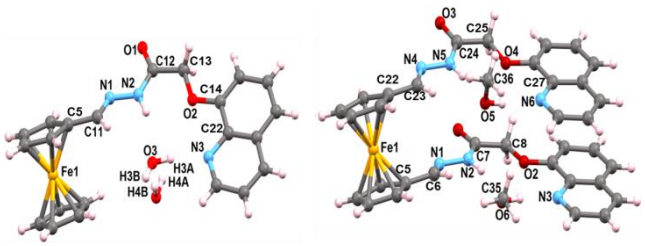

Fig. 1. Molecular structure of receptor **3** and **4**. Selected bond lengths (Å); **3**: C5-C11 1.449(3), C11-N1 1.269(3), N1-N2 1.391(2), C12-N2 1.331(3), C13-O2 1.415(2). **4**: C5-C6 1.447(3), C6-N1 1.272(3), N1-N2 1.389(3), C7-N2 1.342(3), C8-O2 1.426(3), C22-C23 1.452(3).

The X-ray diffraction analysis revealed that compound **3** crystallizes in *P21/c* space group in monoclinic crystal system, where two water molecules are H-bonded with the nitrogen atoms of quinoline and hydrazine unit and forms a 3D water network in a helical array (Fig.1). On the other hand, compound **4** crystallizes in *P-1* space group in triclinic crystal system and shows presence of discrete methanol molecules inside its cavity. To avoid steric interaction between the ferrocene moieties of two successive title molecules, they exist in the opposite orientation in compound **3** (Fig.2). Moreover, each semicircular molecule generates an extended 3D coordination framework having central channels with a cross-section of ca.14.8×14.8 $Å^2$ along the *c* axis. The water molecules O_1W and O_2W interact with their symmetry-related water molecules through two O–H···O hydrogen bonds to form 1D helical water chain parallel to *a*-axis (Fig.3a). It is worth noting that the lattice water molecules form an infinite one dimensional array in a helical manner and this water chain was stabilized by intermolecular hydrogen bonds. The average O···O distance in the helical water chains (2.788 Å)

is in good agreement with reported water clusters,[17,18] however, 0.03Å longer than the corresponding value in hexagonal ice (ice Ih, 2.759 Å) and 0.06 Å shorter than the liquid water (2.854 Å). These comparable distances might be attributed from the compact environment, where hydrogen-bonding interactions present in the units drive the water molecules closer. The crystal structure of **3**

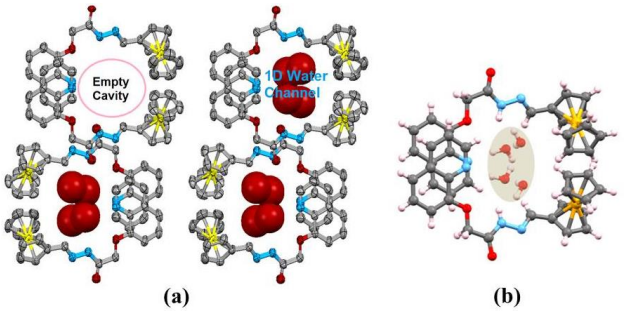

Fig. 2. (a) Three dimensional crystal lattice of compound **3** along *c* axis showing the cavity which holds the water molecules in a helical manner; (b) extended view along *c*-axis with water molecules in the cavity.

was stabilized *via* intramolecular N–H···O, C–H···O, O–H···O, and O–H···N hydrogen bonds (Fig.S9)†. In addition, the packing is further stabilized by $\pi\cdots\pi$ and C-H···π interactions. The inclusive structural design of **3** articulates the interlayer hydrophilic 1D networks that run parallel to the *a* axis. These hydrophilic networks are filled with lattice water molecules (two per unit cell) forming both left-handed and right-handed helices inside the cavities of crystal lattice (Fig.3a-c). The interaction between these lattice waters produced an extended network of H bonds along the 1D chain and therefore, provides a potential proton transfer pathway. On the other hand, in compound **4** methanol molecules occupied the void space in the crystal lattice, which are arranged in discrete 1D chains (Fig.3d).

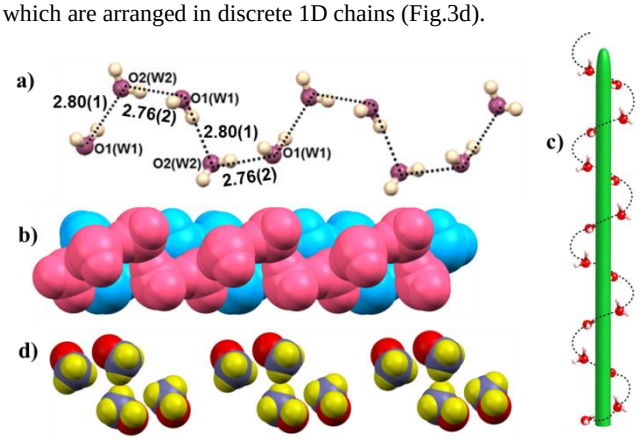

Fig. 3. (a) Water to water interaction, (b) space-fill illustration of both right and left handed water helices, (c) axis passed through helical array (d) 1D discrete methanol chain in **4** parallel to *b*-axis.

To understand the packing arrangement of **3**, the 3D networks have been shown along *c*-axis (Fig.4). Along the *c*-axis, molecules are arranged like walls (Fig.S9)† and each wall exists due to the presence of three different interactions i.e. C–H···O, C-H···π and $\pi\cdots\pi$ stacking. Similarly, the hydrogen bonding analysis for **4** showed that the methanol molecules present in the crystal lattice occupied the void spaces and adopted an interesting zigzag network. The methanol oxygen atoms and the oxygen and nitrogen atoms of **4** take part in various N-H···O, C-H···O interactions (Figs.S10-S12)†. The molecules are self-assembled through hydrogen bonded network in such a way that they can arrange themselves in parallel sheets through *ac* plane. The 2D sheets are further arranged into 3D framework through π–π stacking interactions and some other weak C-H···O interactions.

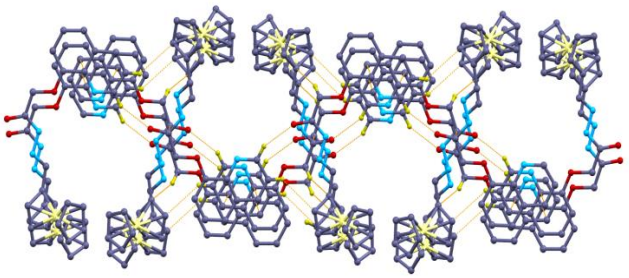

Fig. 4. Intermolecular C-H···O and C-H···π interactions in **3** in 3D networks along *c*-axis (hydrogen atoms except the interacted one and solvent molecules are removed for clarity), Colour code: Fe: yellow; C: violet; N: cyan; O: scarlet red; H: light green.

In order to provide further evidence of water affinity apart from crystallographic information, reversibility of dehydration and rehydration of **3** was performed using thermo gravimetric analysis (TGA) and IR spectroscopy. The TGA analysis shows a clear weight loss of about 9.044% in the temperature range of 90 to 140 °C, which is attributed to the loss of two water molecules per formula (Fig.S13)†. The dehydrated polycrystalline compound was exposed to water vapour that shows crystalline nature within 16-20 h, which is confirmed by IR (Fig.5).[19] In compound **3**, water escapes at 90 ˚C, while in **4** the same phenomenon occurs at higher temperature (~200 ˚C) (Fig.S14)†. This may be due to the encapsulation of methanol molecules in **4**.

It has been observed that compounds containing water chains and clusters inside the framework facilitate proton conduction.[10] This encouraged us to investigate the proton conductivity of **3** in solid state. Indeed, **3** showed good proton conductivity (2.9×10^{-6} S cm^{-1} at 120 °C and 98% RH) due to the presence of helical water chain with activation energy comparable to that of Nafion. It is to be noted that the proton conductivity of organic polymers with sulfonic acid, like Nafion, is reported to be 10^{-1}-10^{-5} S cm^{-1}, while for other acidic functional groups it is different, such as, 10^{-1}-10^{-4} for phosphate, 10^{-5}-10^{-6} for carboxylic acid and 10^{-6}-10^{-8} S cm^{-1} for imidazole.[20, 21]

The temperature-dependent proton conductivities of **3** were measured at RH 98% (Fig.6) that showed a gradual increase in proton conductivity with an increase in temperature from RT to 120 °C. The activation energy (Ea) of proton conductivity was calculated to be 0.30 eV from the least-squares fits of the slopes (Arrhenius plot) (Fig.S15)†. This value is significantly comparable to that of Nafion (Ea = 0.22 eV). Therefore, the mechanism of proton conductivity of **3** follows the Grotthuss[22] hopping mechanism (Ea = 0.1-0.4 eV), not by vehicle mechanism[23] (Ea = 0.5-0.9 eV).

Recently, we have reported a number of ferrocene based efficient redox-active chemosensors for metal recognition, where

polycyclic hydrocarbon viz anthracene, pyrene, cholesterol, benzylacetate etc have been incorporated.[15,16] Interestingly, compound **3** and **4** also contains ferrocene and a heterocyclic moiety (quinoline) that has the potential to sense metal ions. As a result, we investigated the cation recognition properties of **3** and **4** that showed significant switching-on fluorescent response and changes in its electrochemical behaviour upon addition of Zn^{2+} (Fig. S16)†. The absorption response behavior of the compounds were investigated in presence of various metal salts (Na^{+}, Ca^{2+}, Mn^{2+}, Ni^{2+}, Co^{2+}, Fe^{2+}, Tl^{+}, Hg^{2+}, Cd^{2+} and Pb^{2+}) in CH_3CN/water (1:9) (Fig. S17)†. Upon addition of Zn^{2+} ion into an aqueous solution of **3** and **4** showed a new maximum absorption band at 233 and 235 nm respectively (Figs. S16 and S17)†. Both the solutions exhibited a characteristic colour change from yellow to orange (Fig. S18)†. The UV−vis absorption spectrum of **3** in water showed a blue shift from 240 nm ($\varepsilon = 270 \times 10^3\ M^{-1}\ cm^{-1}$) to 233 nm ($\varepsilon = 266 \times 10^3\ M^{-1}\ cm^{-1}$) upon gradual addition of Zn^{2+} ion (Fig. S16)†. On the other hand, **4** showed a red shift in the spectral position at 235 nm along with a decrease in the absorption intensity (Fig. S17)†. A very well defined isosbestic points were obtained at 252 and 323 nm, indicating only one spectrally distinct complex. The binding assays using the method of continuous variations (Job's plot) suggest 1:1 (cation/receptor) complex formation with Zn^{2+} ion both for **3** and **4** (Figs. S19, S20)†. Further, the stoichiometries of these complexes have been confirmed by ESI-MS (Figs. S21, S22)†. The binding constant values towards Zn^{2+} have been determined from the increasing absorption intensity and was found to be K (±15%) = 2.55×10^4 for **3** at (at λ_{max}= 205 nm) and $2.89 \times 10^4\ M^{-1}$ for **4** (at λ_{max}= 202 nm) (Figs. S23, S24)†.

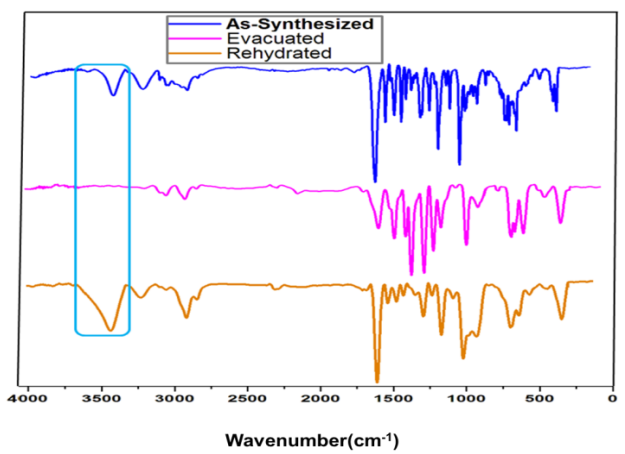

Fig. 5. Reversible transformation of water peaks in IR spectra of compound **3**.

The effect of Zn^{2+} on the fluorescence intensities of receptors **3** and **4** was tested by fluorescence spectroscopy (Fig. 7). Both the receptors show moderate fluorescence in water ($c = 1.0 \times 10^{-7}$ M) when excited at λ_{exc} = 292 nm for **3** and at λ_{exc}= 295 nm for **4**. Upon addition of various metal ions to a solution of **3**, only Zn^{2+} showed a strong enhancement of fluorescence with a spectral shift from 402 nm to 417 nm (CHEF = 15) (Figs. S25, S26)†. Similarly, receptor **4** shows 18 fold enhancement upon coordination with Zn^{2+} ion (Fig. S27)†. Selective fluorescence enhancement observed in **3** could be due to the effective coordination of Zn^{2+} with nitrogen atom of the fluorophore as well as imine functionality of **3**. This restricts the PET[24] process and enhances the fluorescence output of **3** via chelation induced fluorescence enhancement. Detection limit was calculated to be ~2 ppb (Fig. S28)† and the binding constant values of **3** and **4** with Zn^{2+} ion have also been determined following the modified Benesi–Hildebrand equation[25] and the values are in the same order as obtained from UV-vis data. The reversible interaction for receptors **3** and **4** with Zn^{2+} was confirmed by an extraction experiment (Figs. S29, S30)†.

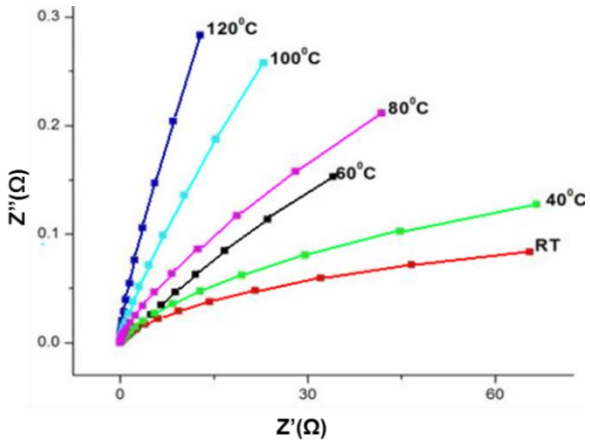

Fig. 6. Plot of the complex impedance plane for compound **3** at various temperatures at 98% RH.

The metal-recognition properties of receptors **3** and **4** were also evaluated by cyclic voltammetry (CV) and differential pulse voltammetry (DPV) analysis in (CH_3CN/H_2O, 1/9) solutions containing 0.1 M $[(n\text{-}Bu)_4N]ClO_4$ as supporting electrolyte. Receptors **3** and **4** displayed a reversible one-electron oxidation process at $E_{1/2}$ = 0.59 V and $E_{1/2}$ = 0.63V respectively (Figs. S31, S32)† due to the ferrocene/ferrocenium redox couple. However, the original peak gradually decreased upon stepwise addition of Zn^{2+} ions and a new peak, associated with the formation of a complex species appeared at 0.66 V for **3**, 0.72 V for **4**, respectively, (Figs. S33, S34)†. The linear sweep voltammetry study (LSV) (Figs. S35, S36)† further reveals similar results as obtained from CV and DPV. The ^1H NMR titration experiments (Fig. S37)† were further performed to gain detailed information about the binding interactions of Zn^{2+} ions by receptors **3** and **4** (Scheme S2)†.

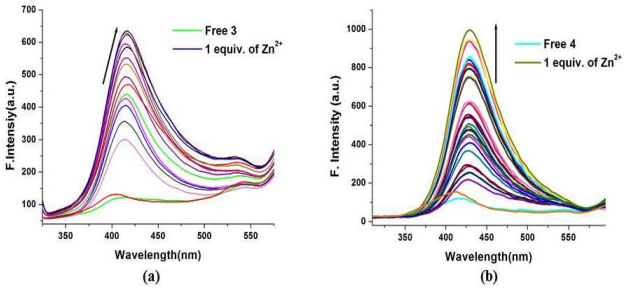

Fig. 7. Fluorescene emission change of **3** (a) (1.0×10^{-7} M) and **4** (b) (1.0×10^{-7} M) (right) upon addition of Zn^{2+} ion upto 1 equivalent in water.

In conclusion, we report the synthesis and structural characterization of two ferrocene-quinoline conjugates **3** and **4**. Compound **3** shows internal H-bonding networks that act as efficient proton conducting pathways and exhibits high proton conductivity at elevated temperature *via* 1D helical water chain. Activation energy, derived from an Arrhenius plot, suggests that the proton conduction in **3** occurs through Grotthuss mechanism. In addition, both the conjugates have been shown to detect efficiently biologically important Zn^{2+} ion in water with a detection limit of 2 ppb.

Notes and references

[a]*Department of Chemistry, Indian Institute of Technology Madras, Chennai (600036), India.*
[b]*Physical Chemistry Division, CSIR National Chemical Laboratory, Pune, 411008, India*
Fax: 91-44-2257 4202; Tel: 91-44-2257 4230; E-mail: sghosh@iitm.ac.in

Generous support of the Department of Science and Technology, DST (Project No. SR/SI/IC-31/2011), New Delhi, India is gratefully acknowledged. J.P.S and S.K.B. thanks to IIT Madras for research fellowships.

† Electronic Supplementary Information (ESI) available: Experimental details, X-ray analysis details, ^{1}H, ^{13}C NMR and ESI-MS data of **3** and **4**, UV−vis data, Fluorescence data, CV data, ESI-MS spectra of **3** and **4** with Zn^{2+}. Crystallographic information (CIF) for compound **3** and **4**. CCDC No. for compound **3** is 1018549 and **4** is 1018535. See DOI: 10.1039/c000000x/†

1. (a) A. A.-Sato, H. Akutsu, S. S. Turner, P. Day, M. R. Probert, J. A. K. Howard, T. Akutagawa, S. Takeda, T. Nakamura and T. Mori, *Angew. Chem., Int. Ed*., 2005, **44**, 292; (b) Proton Conductors: Solids, Membranes and Gels-Materials and Devices. Series: Chemistry of Solid State Materials, 2nd ed.; Colomban, P., Ed.; Cambridge University Press: Cambridge, UK, 1992.
2. (a) P. Ramaswamy, R. Matsuda, W. Kosaka, G. Akiyama, H. J. Jeon and S. Kitagawa, *Chem. Commun*., 2014, **50**, 1144; (b) D. Samanta and P. S. Mukherjee, *Chem. Commun*., 2014, **50**, 1595; (c) D. Samanta and P. S. Mukherjee, *Chem. Eur. J*., 2014, **20**, 5649.
3. J. Surowiec and R. Bogoczek, *J. Therm. Anal*., 1998, **33**, 1097.
4. J. M. Taylor, R. K. Mah, I. L. Moudrakovski, C. I. Ratcliffe, R. Vaidhyanathan and G. K. H. Shimizu, *J. Am. Chem. Soc*., 2010, **132**, 14055.
5. (a) S. C. Sahoo, T. Kundu and R. Banerjee, *J. Am. Chem. Soc*., 2011, **133**, 17950; (b) T. Panda, T. Kundu and R. Banerjee, *Chem. Commun*., 2013, **49**, 6197; (c) S. S. Nagarkar, S. M. Unni, A. Sharma, S. Kurungot and S. K. Ghosh, *Angew. Chem., Int. Ed*., 2013, **53**, 2638; (d) S. Saha, E. -M. Schon, C. Cativiela, D. D. Diaz and R. Banerjee, *Chem. Eur. J*., 2013, **19**, 9562.
6. (a) M. Sadakiyo, T. Yamada and H. Kitagawa, *J. Am. Chem. Soc*., 2009, **131**, 9906; (b) T. Yamada, M. Sadakiyo and H. Kitagawa, *J. Am. Chem. Soc*., 2009, **131**, 3144; (c) A. Shigematsu, T. Yamada and H. Kitagawa, *J. Am. Chem. Soc*., 2012, **134**, 13145.
7. (a) E. Fabbri, D. Pergolesi and E. Traversa, *Chem. Soc. Rev*., 2010, **39**, 4355; (b) H. Iwahara, H. Uchida and N. Maeda, *Solid State Ionics*, 1983, **11**, 109.
8. (a) H.-R. Xu, Q.-C. Zhang, H.-X. Zhao, L.-S. Long, R.-B. Huang and L.-S. Zheng, *Chem. Commun*., 2012, **48**, 4875; (b) G. K. H. Shimizu, R. Vaidhyanathan and J. M. Taylor, *Chem. Soc. Rev*., 2009, **38**, 1430.
9. J. F. Nagle, Proton transport in condensed matter, in Proton Transfer in Hydrogen-Bonded Systems, ed. T. Bounties, Plenum press, New York, 1992.
10. (a) A. Mukherjee, M. K. Saha, M. Nethaji and A. R. Chakravarty, *Chem. Commun.*, 2004, 716; (b) B. S. Kumar and P. K. Panda, *Cryst. Eng. Comm.*, 2014, **16**, 8669.
11. Ferrocenes, Homogeneous Catalysis, Organic Synthesis, Material Science (Eds.: A. Togni, T. Hayashi), VCH, Weinheim 1995.
12. M. S. Boroglu, S. U. Celik, I. Boz and A. Bozkurt, *J. Mater. Res.*, 2013, **28**, 1458.
13. S. G-. Focil, R. C. Woudenberg, O. Yavuzcetin, M. T. Tuominen and E. B. Coughlin, *Macromolecules*, 2007, **40**, 8708.
14. H. Yang, Z. Zhou, K. Huang, M. Yu, F. Li, T. Yi, and C. Huang, *Org. Lett.*; 2007, **9**, 4729.
15. (a) A. Thakur, D. Mandal and S. Ghosh, *Anal. Chem*., 2013, **85**, 1665; (b) A. Thakur and S. Ghosh, *Organometallics* 2012, **31**, 819; (c) A. Thakur, D. Mandal, P. Deb, B. Mondal and S. Ghosh, *RSC Adv.*, 2014, **4**, 1918; (d) A. Thakur, S. Sardar and S. Ghosh, *Inorg. Chem.* 2011, **50**, 7066.
16. (a) D. Mandal, P. Deb, B. Mondal, A. Thakur, S. J. Ponniah and S. Ghosh, *RSC Adv*., 2013, **3**, 18614; (b) S. J. Ponniah, S. K. Barik, A. Thakur, R. Ganesamoorthi and S. Ghosh, *Organometallics* 2014, **33**, 3096.
17. J. K. Gregory, D. C. Clary, K. Liu, M. G. Brown and R. J. Saykally, *Science*, 1997, **275**, 814.
18. S. K. Ghosh and P. K. Bharadwaj, *Inorg. Chem*., 2005, **44**, 5553.
19. Compound **3** shows reversible crystallization by readily reabsorbing moisture and both the frameworks **3** and **4** are stable after removal of water or methanol.
20. (a) G. H. Li, C. H. Lee, Y. M. Lee and C. G. Cho, *Solid State Ionics*, 2006, **177**, 1083; (b) B. Karadedeli, A. Bozkurt and A. Baykal, *Physica B: Condensed Matter*, 2005, **364**, 279.
21. (a) K. A. Mauritz and R. B. Moore, *Chem. Rev*., 2004, **104**, 4535; (b) R. C. Woudenberg, O. Yavuzcetin, M. T. Tuominen and E. B. Coughlin, *Solid State Ionics*, 2007, **178**, 1135.
22. (a) Colomban, P. Proton Conductors: Solids, Membranes and Gels Materials and Devices.Chemistry of Solid State Materials; Cambridge University Press: Cambridge, U.K., 1992; Vol. 2; (b) N. Agmon, *Chem. Phys. Lett*., 1995, **244**, 456; (c) M. Yoon, K. Suh, S. Natarajan, K. Kim, *Angew. Chem*., 2013, **125**, 2752; *Angew. Chem., Int. Ed*., 2013, **52**, 2688; (d) T. Yamada, K. Otsubo, R. Makiura and H. Kitagawa, *Chem. Soc.Rev*., 2013, **42**, 6655; (e) A. S. Nowick and Y. Du, *Solid State Ionics*, 1995, **77**, 137.
23. K. D. Kreuer, A. Rabenau and W. Weppner, *Angew. Chem., Int. Ed*., 1982, **21**, 208.
24. (a) Photoinduced Electron Transfer; M. A. Fox and M. Chanon, Eds.; Elsevier, 1988; (b) R. S. Davidson, *Advances in Physical Organic Chemistry*, 1983, **19**, 1.
25. H. A. Benesi and J. H. Hildebrand, *J. Am. Chem. Soc*., 1949, **71**, 2703.